Received: 22 October 2020 | Revised: 15 November 2020 | Accepted: 17 November 2020

DOI: 10.1002/jmor.21303

RESEARCH ARTICLE

JOURNAL OF morphology WILEY

A postlarval instar of *Phoxichilidium femoratum* (Pycnogonida, Phoxichilidiidae) with an exceptional malformation

Georg Brenneis[1,2,3] | **Gerhard Scholtz**[3]

[1]Cytologie und Evolutionsbiologie, Zoologisches Institut und Museum, Universität Greifswald, Greifswald, Germany

[2]Neuroscience Program, Wellesley College, Wellesley, Massachusetts

[3]Vergleichende Zoologie, Institut für Biologie, Humboldt-Universität zu Berlin, Berlin, Germany

Correspondence
Georg Brenneis, Cytologie und Evolutionsbiologie, Zoologisches Institut und Museum, Universität Greifswald, Greifswald, Germany.
Email: georg.brenneis@gmx.de; gerhard.scholtz@rz.hu-berlin.de

Funding information
Deutsche Forschungsgemeinschaft, Grant/Award Numbers: BR5039/1-1, BR5039/2-1, BR5039/3-1; National Science Foundation, Grant/Award Number: NSF-IOS-1656103

Abstract

Individuals of the marine chelicerate lineage Pycnogonida (sea spiders) show considerable regenerative capabilities after appendage injury or loss. In their natural habitats, especially the long legs of sea spiders are commonly lost and regenerated, as is evidenced by the frequent encounter of specimens with missing or miniature legs. In contrast to this, the collection of individuals with abnormally developed appendages or trunk regions is comparably rare. Here, we studied a remarkable malformation in a postlarval instar of the species *Phoxichilidium femoratum* (Rathke, 1799) and describe the external morphology and internal organization of the specimen using a combination of fluorescent histochemistry and scanning electron microscopy. The individual completely lacks the last trunk segment with leg pair 4 and the normally penultimate trunk segment bears only a single aberrant appendage resembling an extension of the anteroposterior body axis. Externally, the proximal units of the articulated appendage are unpaired, but further distally a bifurcation into two equally developed leg-like branches is found. Three-dimensional reconstruction of the musculature reveals components of two regular leg muscle sets in several of the proximal articles. This confirms interpretation of the entire appendage as a malformed leg and reveals an externally hidden paired organization along its entire proximodistal axis. To explain the origin of this unique malformation, early pioneering studies on the regenerative potential of pycnogonids are evaluated and (a) an injury-induced partial fusion of the developing limb buds of leg pair 3, as well as (b) irregular leg regeneration following near complete loss of trunk segments 3 and 4 are discussed. Which of the two hypotheses is more realistic remains to be tested by dedicated experimental approaches. These will have to rely on pycnogonid species with established laboratory husbandry in order to overcome the limitations of the few short-term regeneration studies performed to date.

KEYWORDS

development, limbs, musculature, Pantopoda, sea spider, regeneration

1 | INTRODUCTION

Pycnogonida (sea spiders) is an old lineage of marine chelicerates that diversified in the Paleozoic and survived with its unmistakable body organization for more than 400 million years until today (Ballesteros et al., 2020; Siveter et al., 2004). Compared to many other arthropods, the pycnogonid trunk is unusually small in relation to its appendages, most prominently among them the anteriorly directed proboscis and (mostly) four pairs of long legs (Arnaud & Bamber, 1987; King, 1973; Figure 1(a),(b)). These are complemented by the anterior cephalic limb pairs, the cheliphores, palps and ovigers, which are borne on the cephalosoma together with the first leg pair of the fused trunk segment 1. The cephalic limbs show considerable structural variations across extant taxa and may be in part or even completely missing in some groups (Figure 1(b)). In contrast, the basic architecture of the legs is remarkably conserved. They are composed of nine articles (coxae 1–3, femur, tibiae 1 and 2, tarsus, propodus and main claw) with characteristic sets of extrinsic and intrinsic muscles. Most articles are equipped with a ventral pair of anterior and posterior depressors and an antagonistic dorsal pair of levators (e.g., Dencker, 1974; Helfer & Schlottke, 1935; Figure 1(c)). Only coxa 1 features anterior protractors and posterior retractors, which mediate the major component of a leg's forward and backward movement, respectively. In addition to the musculature, each leg contains diverticula of the midgut and the gonads, presumably to compensate for space restrictions in the narrow trunk (e.g., Arnaud & Bamber, 1987; Dohrn, 1881; Figure 1(c)). Notably, the midgut diverticula have been shown to also support internal oxygen transport by peristaltic contraction (Woods et al., 2017), as the pycnogonid heart and other structures guiding hemolymph circulation are rather weakly developed (Bogomolova & Malakhov, 2011; Tjønneland et al., 1985). In contrast to most fossil and recent chelicerate taxa, extant pycnogonids lack a prominent opisthosoma (Dunlop & Lamsdell, 2017). Instead, only a small anal tubercle (or so-called abdomen) projects from their last trunk segment (Figure 1(b)). Interpretation of this unsegmented structure as a reduced opisthosoma is widely accepted and supported by fossils placed in the pycnogonid lineage (e.g., Bergström et al., 1980; Poschmann & Dunlop, 2006) and the transient development of supernumerary posterior ganglion anlagen in the central nervous system of extant representatives (e.g., Brenneis & Scholtz, 2014; Brenneis 2016)

Postembryonic development of Pycnogonida has been covered in several classical histological works, which have been complemented by a number of more recent studies (see Brenneis et al., 2017 for review; Alexeeva et al., 2017; Alexeeva et al., 2018, 2019; Brenneis & Arango, 2019; Mochizuki & Miyazaki, 2017). Notably, there are also some reports of abnormally developed postembryonic instars and adult pycnogonid specimens with aberrant shapes of the trunk and the appendages. These malformations show patterns found also in other arthropod groups (e.g., Bateson, 1894; Scholtz, 2020) and include missing or supernumerary legs (Arita, 1936; Bouvier, 1914; Dogiel, 1911; Galli et al., 2019; Ohshima, 1942a), palps and legs with several branches or with fused articles (Gordon, 1932; Ohshima, 1942b; Schimkewitsch & Dogiel, 1913; Scholtz & Brenneis, 2016) and double anal tubercles (Schimkewitsch & Dogiel, 1913).

Regeneration is a widespread phenomenon among metazoans and has attracted the attention of researchers for centuries (e.g., Elliott & Sánchez Alvarado, 2018; Korschelt, 1907; Tiozzo & Copley, 2015; Trembley, 1744). It also occurs in arthropods, where it

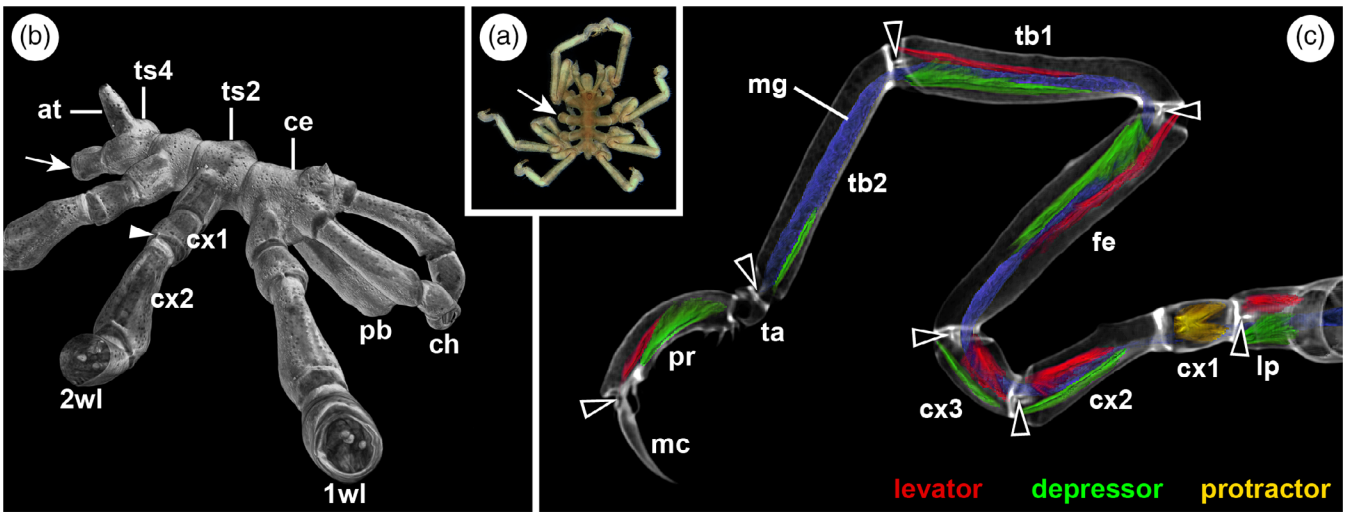

FIGURE 1 External morphology and leg musculature of *Phoxichilidium femoratum*. (a) Dorsal view of adult male (brightfield stereomicroscopy). Arrow indicates missing leg 2. (b) Volume rendering (X-ray micro-computed tomography, μCT scan) of the trunk of an adult female, dorsolateral view, anterior to the right. Note the absence of palps and ovigers. The arrowhead highlights exemplarily the dorsally located joint between coxae 1 and 2 of leg 2. The arrow indicates missing leg 4. The cephalosoma includes trunk segment 1 that bears the first leg pair. (c) Reconstruction of the intrinsic and extrinsic musculature of leg 3 of an adult male (μCT scan), anterior view. Note the typical arrangement of ventral depressors (green) and dorsal levators (red) in the lateral process, coxae 2 and 3, femur, tibia 1 and propodus. The tibia 2 lacks the dorsal levators. The tarsus and main claw contain no intrinsic musculature. The coxa 1 is the only article with anterior protractors (yellow) and posterior retractors (not visible, covered by protractors). Open arrowheads indicate lateral joints between articles. at, anal tubercle; ce, cephalon; ch, cheliphore; cx, coxa; fe, femur; lp, lateral process; mc, main claw; pb, proboscis; pr, propodus; ta, tarsus; tb, tibia; ts, trunk segment; wl, walking leg

is primarily restricted to the regeneration of limbs after injury and/or autotomy (e.g., Charmantier-Daures & Vernet, 2004; Marruzo & Bortolin, 2013; Maruzzo et al., 2005; Przibram, 1909). Pycnogonids are no exception to this and specimens with missing or smaller regenerating legs have been repeatedly documented (Dohrn, 1881; Gaubert, 1892; Hedgpeth, 1947; Helfer & Schlottke, 1935; Loeb, 1895; Maruzzo et al., 2005; Schimkewitsch & Dogiel, 1913; Figure 1(a),(b)). Hence, it is reasonable to assume that most cases of malformation reports in sea spiders are due to aberrant regeneration processes and perturbations during embryonic or postembryonic development (Scholtz & Brenneis, 2016).

Here, we describe a unique malformation pattern in an advanced postlarval instar of the pycnogonid species *Phoxichilidium femoratum* (Rathke, 1799). The individual lacks trunk segment 4 and its legs. Trunk segment 3 is reduced in size and possesses a single malformed leg-like appendage that is, however, perfectly aligned with the anteroposterior body axis and features partially paired external structures. To better understand the underlying architecture of the aberrant structure, we also studied its internal organ systems, with particular focus on the musculature. The unusual malformation is discussed in comparison to other abnormal patterns in pycnogonids and hypothetical scenarios how this malformation came into being are provided.

2 | MATERIAL AND METHODS

2.1 | Specimen collection and fixation

Specimens of *Phoxichilidium femoratum* (Rathke, 1799) were collected close to Prescott Park in Portsmouth, NH, USA, in June and July 2015, July 2017 and 2018, and September 2019 (Figure 1(a)). In the summer months, adults and the free-living developmental instars of *P. femoratum* cling to and feed on the hydrozoan *Ectopleura larynx* (Ellis and Solander, 1786); syn. *Tubularia larynx*). Patches of the hydrozoan colonies were removed from floating docks and transferred into sea water tanks filled with artificial sea water in the Animal Care Facility at Wellesley College. Small pieces of the hydrozoan colonies were checked under a stereomicroscope and pycnogonids manually removed. The malformed specimen of *P. femoratum* was found among numerous normally developed postlarval, juvenile and adult specimens (terminology following Brenneis et al., 2017). In addition to these free-living instars, also a handful of earlier endoparasitic stages were dissected from infested polyps. Samples were fixed overnight in 4% paraformaldehyde in phosphate-buffered saline (PFA/PBS, Boston BioProducts #BM-155) at 4°C. Fixation was followed by thorough rinsing in PBS (75 mmol l^{-1} Na_2HPO_4, 20 mmol l^{-1} KH_2PO_4, 100 mmol l^{-1} NaCl, pH 7.4) and storage at 4°C for a few days.

2.2 | Fluorescent histochemistry

Prior to staining of the malformed individual, tissue permeability was improved by incubation in PBTx (PBS + 0.3% Triton X-100) for two hours with several changes of the buffer. F-actin labeling for visualization of the musculature was performed with A488-conjugated phalloidin (Invitrogen Molecular Probes® #A12379, 1:50 in PBTx) overnight at 4°C. After rinsing in several changes of PBS at room temperature (RT), DRAQ5™ (BioStatus #DR50050, 5 μmol l^{-1} in PBS; RRID:AB_2314341) was used for nuclear counterstaining. The specimen was subsequently cleared in Vectashield® Mounting Medium (Vector Laboratories, Inc. #H-1000; RRID:AB_2336789) and mounted on a microscopic slide with tiny plasticine pieces attached to the corners of the cover slips to prevent its compression. During data acquisition, the signal intensity of DRAQ5 in the nuclei was observed to diminish rapidly, with simultaneous leakage into the surrounding tissue, resulting in a diffuse labeling. This observation was subsequently confirmed with further samples to occur whenever DRAQ5-labeled tissues were transferred into glycerol-based mounting media. For the malformed specimen, additional nuclear labeling using Hoechst (H33342, Invitrogen Molecular Probes® #H1399, 1 μg/mL in PBS) was attempted, incubation lasting two hours at RT with gentle agitation on a horizontal shaker. Identical staining procedures (Hoechst + phalloidin) were thereafter performed for normally developed specimens.

2.3 | Confocal laser-scanning microscopy and data analysis

Confocal laser-scanning microscopy (CLSM) was performed with a Leica DMI 6000 CS microscope coupled to a Leica TCS SP5 II scan unit. Based on the excitation spectra of the fluorochromes, a combination of UV laser (405 nm wavelength → Hoechst & cuticular autofluorescence), argon laser (488 nm wavelength → A488-phalloidin) and helium-neon laser (633 nm wavelength → DRAQ5) was selected.

The software package Amira (version 5.6; FEI Visualization Sciences Group; RRID:SCR_007353) was used for data analysis and visualization. Texture-based 3D-volume rendering ("Volren" module, "VRT" mode) with specular shading was employed to visualize musculature, cuticular autofluorescence and nuclear labeling. In some cases, VRT and maximum intensity projection ("MIP") modes were combined for depiction of muscles and nuclei. Filtered oblique slicers were used to remove nontarget structures covering the view at regions of interest. Differential coloration of musculature was achieved via manual 3D-segmentation of multiple materials in one label field and subsequent referencing of the data channels to this label field with specification of differently colored transfer functions for different materials.

2.4 | Scanning electron microscopy (SEM)

Following CLSM imaging, the malformed specimen was thoroughly rinsed in PBS, transferred back to PFA/PBS and stored at 4°C for several months. Thereafter, it was dehydrated in a graded ethanol series (15%, 30%, 50%, 60%, 70%, 80%, 90%, 96%, 2x 100%, each step at least 30 min at RT), critical point-dried with a Bal-Tec CPD 030 and sputtered with gold using a Bal-Tec SCD 005. Micrographs were taken with a Zeiss LEO 1430 scanning electron microscope.

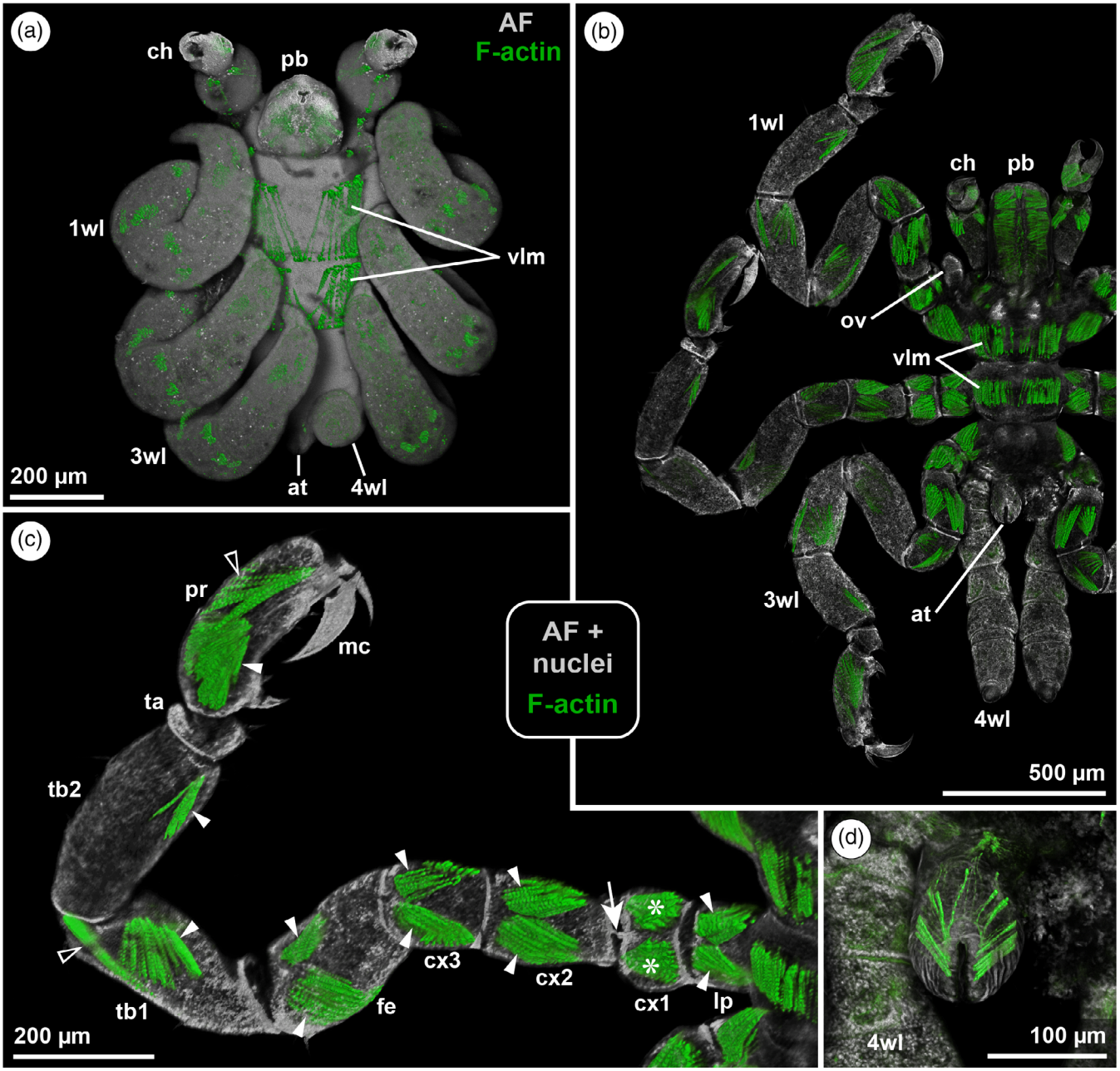

FIGURE 2 Late endoparasitic and first free-living instars of *P. femoratum*. Volume renderings (CLSM scans) showing F-actin labeling (green) together with nuclear counterstain and/or cuticular autofluorescence (gray). (a) Late endoparasitic instar dissected from the hydrozoan host, ventral view. Note elongate limb buds of leg pairs 1–3 and small bud of leg pair 4 flanking the posterior anal tubercle. Formation of ventral longitudinal muscles in trunk segments 1 and 2 and of the leg musculature has been initiated. (b) First free-living instar after emergence from the hydrozoan host. Male with oviger anlage, ventral view. Note functional leg pairs 1–3 and elongate, externally unarticulated limb buds of leg pair 4 with internal regionalization into the prospective leg articles. The ventral longitudinal muscles of trunk segment 3 are not yet differentiated. (c) Intrinsic musculature of leg 2, posteroventral view (leg slightly flattened under cover slip to facilitate documentation). Note well-developed anterior and posterior depressor muscles (solid arrowheads) in coxae 2 and 3, femur and tibia 1 and propodus (latter two articles seen laterally), whereas tibia 2 possesses only relatively weak depressors. Open arrowheads mark levators in tibia 1 and propodus. Coxa 1 is the only article with anterior protractor and posterior retractor muscles (asterisks) and an accompanying 90° rotation of the joints with coxa 2 (arrow). Proximally, paired depressors of extrinsic leg musculature in the lateral process (solid arrows) are visible. (d) Detail of the anal tubercle with increased signal intensity of F-actin labeling to visualize the muscle bundles mediating the opening of the slit-shaped anus. AF, autofluorescence; at, anal tubercle; ch, cheliphore; cx, coxa; fe, femur; lp, lateral process; mc, main claw; ov, oviger anlage; pb, proboscis; pr, propodus; ta, tarsus; tb, tibia; vlm, ventral longitudinal trunk musculature; wl, walking leg

2.5 | X-ray micro-computed tomography

Adults of *P. femoratum* were fixed in Bouin's fluid (10% formaldehyde, 5% glacial acetic acid in saturated aqueous picric acid). Specimens were thoroughly rinsed in PBS, transferred into deionized water, slowly dehydrated via an ascending ethanol series and incubated in a solution of 2% iodine (resublimated; Carl Roth; #X864.1) in 99.5% ethanol for ca. 48 hours at ambient temperature. After rinsing in 99.5% ethanol (3-4x 10 min) they were critical point-dried using a Leica EM CPD300 and placed in 1.7 mL Eppendorf tubes glued with their tips to plastic welding rods. Scans were performed with an Xradia MicroXCT-200 (Carl Zeiss Microscopy) under 40 kV/200 μA/8 W, using a 4x objective, 1.25–1.75 s exposure times, and "binning 2" to reduce noise. Tomography projections were reconstructed with the XMReconstructor software (Carl Zeiss Microscopy) with "binning 1" (= full resolution) and TIFF format image stacks as output. Processing and 3D-visualization of the image stacks was done using Amira as described above.

2.6 | Data presentation

Adobe Photoshop CS5 (version 12.1.0; RRID:SCR_014199) was used to adjust global contrast and brightness values of images and to merge the SEM micrographs showing the overview of the malformed specimen. All figures were compiled with Adobe Illustrator CS5 (version 15.1.0; RRID:SCR_010279). If not noted otherwise, specimens and structures are shown with anterior pointing to the top.

3 | RESULTS

3.1 | A short summary of phoxichilidiid postembryonic development and collection success

Deviating from most other pycnogonids, phoxichilidiid species spend a significant part of their postembryonic development as endoparasitic instars in hydrozoans (Adlerz, 1888; Dogiel, 1913; Dohrn, 1881; Lebour, 1916, 1945; Lovely, 2005; Maxmen, 2006). They hatch as a protonymphon larva with modified filamentous distal podomeres of the palpal and ovigeral larval legs, which are most likely apomorphic for the group (Brenneis et al., 2017). The larva attaches to a hydrozoan and the second instar penetrates into the gastrovascular cavity (Maxmen, 2006) where it passes through several molts and three pairs of long legs are formed with a flat anteroposterior developmental gradient (Figure 2(a)). After a final endoparasitic molt, the first free-living instar emerges from its host, bearing three functional leg pairs and externally unarticulated buds of leg pair 4 (Figure 2(b)). At this stage, the three anterior legs have attained the characteristic nine-articled structure, although the articles are still proportionately shorter than in the adult (Figures 1(c) and 2(b)). The extrinsic and intrinsic leg muscle sets are fully differentiated (Figure 2(c)). Furthermore, a complete through-gut is present, terminating in a muscular slit-shaped anus at the tip of the anal tubercle (Figure 2(d)).

In the four years of specimen collection, several hundred first free-living instars together with similar numbers of more advanced juveniles and adults were obtained from the hydrozoan colonies. Individuals with partially or completely missing legs were commonly encountered (e.g., Figure 1(a),(b)).

3.2 | The malformed specimen: Live observation and external morphology

The aberrant postlarval instar was found in June 2015, its malformation being the only of its kind in the material collected over four summers, indicating a rare occurrence of this type of abnormal development in *P. femoratum*. The individual was briefly observed while being kept alive in a petri dish with sea water. It moved actively and clung to pieces of hydrozoan stolons placed in the dish.

Only the first two leg pairs of the specimen are normally developed (Figure 3(a)) showing the characteristic nine-articled composition and emanating from laterally protruding processes of their corresponding trunk segments (compare Figures 1(c), 2(c), and 3(b)). Likewise, the position of the joints between the articles of the first two leg pairs conforms with the regular pattern, including their rotated ventral and dorsal placement between coxae 1 and 2, as opposed to lateral positions in all other cases (compare Figures 1(b),(c) and 3(b)). Conspicuously, trunk segment 3 bears only a single aberrant appendage that is directed posteriorly, whereas no traces of trunk segment 4 and its leg pair are found (Figure 3(a)). Prior to fixation, the specimen was observed to hold the aberrant appendage for most of the time elevated from the substrate (similar to Figure 3(a),(d)). In correspondence to regular legs, it is articulated into nine units along its proximodistal axis. The five proximal units are unpaired and bear some resemblance to regular leg articles, although articles 4 and 5 ("femur" and "tibia 1") are slightly shorter (Figure 3(a),(d)). First indications of a paired organization become apparent with the next article ("tibia 2"), which widens from proximal to distal and shows a slight median depression at its distal margin (Figure 3(c)). From there on, two completely separated regular sets of the three unmistakable distal leg articles (tarsus, propodus and main claw) project distally (Figure 3(a),(c)), thereby providing evidence that the aberrant appendage represents at least partially a malformed leg. The joints between the leg articles were not readily discernible in SEM micrographs (see Figure 3(d)), but cuticular autofluorescence reveals the presence of at least some lateral joints (Figures 4(a) and 6(a)). Most conspicuously, a pair of ventral joints is found between "coxa 1" and "coxa 2", contrasting to a single joint found in a regular leg in this position (Figure 4(b)). At the opposite dorsal side, joints are not developed (Figure 4(c)). In regular legs, femur and tibiae 1 and 2 each bear a prominent dorsodistal seta (Figures 3(a) and 4(a)). In the malformed appendage, a pair of similarly long setae is found only at the dorsodistal margin of the abnormally shaped "tibia 2", while they are absent on the "femur" and "tibia 1" (Figures 3(c),(d) and 4(a)).

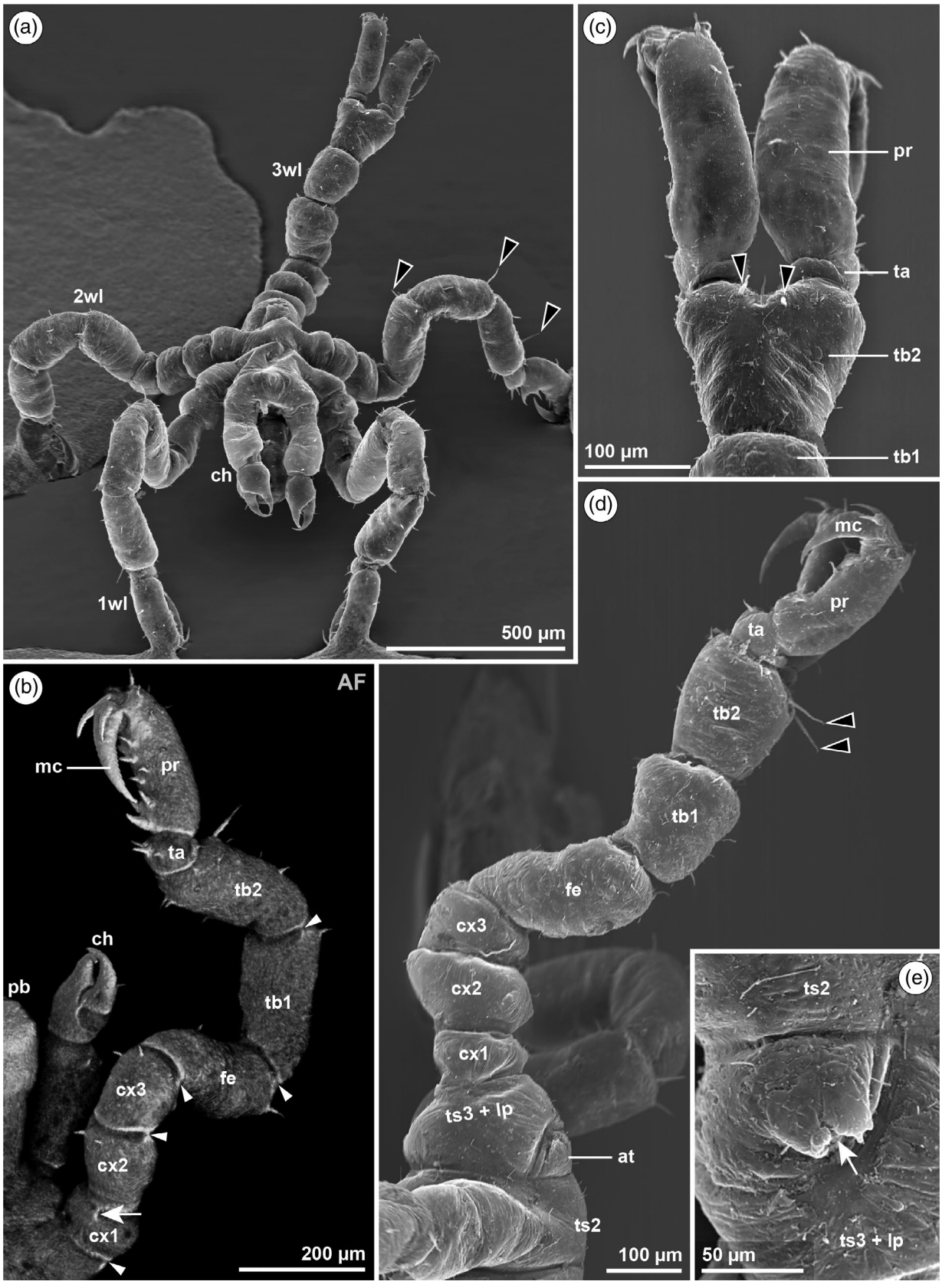

FIGURE 3 Legend on next page.

At the dorsal segment border of trunk segments 2 and 3, a small anal tubercle-like protrusion is found (Figures 3(d),(e) and 4(c)). At its posterior tip, it features an inconspicuous slit-like depression of the cuticle, but a proper opening is not apparent (Figure 3(e)).

3.3 | Musculature of the malformed specimen

The muscles in the proboscis, the cheliphores, and the first two leg pairs are normally differentiated (Figure 4(a),(a')). Likewise, the ventral and dorsal longitudinal musculature between the trunk segments is developed as in a regular first free-living instar. As is characteristic for Phoxichilidiidae (Dohrn, 1881), the ventral trunk musculature is much more pronounced than its dorsal counterpart (Figure 4(a),(a')). There is a distinct separation of the dorsal longitudinal muscle bundles, which are found in a far lateral position (Figure 4(c)). This is presumably due to the mediodorsally located longitudinal heart (not visible in our data).

In the proximal articles of the malformed appendage, the ventral extrinsic and intrinsic musculature resembles not one, but essentially two regular leg muscle sets per article, being developed in the respective left and right body halves. This observation aligns with the ventral double joints between "coxa 1" and "coxa 2" in revealing a paired organization underlying the externally unpaired-looking proximal articles. Further, it unequivocally proves that the appendage represents a malformed leg along its entire length. According to its unusual anteroposterior orientation, the lateral and medial muscle groups of the malformed leg correspond to the anterior and posterior muscles sets, respectively, of a regular leg. (Figure 4(b)).

The ventral extrinsic leg musculature is not as sorted as in a regular lateral process. Nonetheless, the fan-shaped arrangement of depressors remains recognizable in each body half (i.e., "posterior" muscle bundle at least partially formed; Figure 2(c) for normal arrangement). "Coxa 1" features only marginally developed retractors at the ventral midline, medial to the double joints (Figure 4(b)). "Coxa 2" and "coxa 3" are equipped with distinctly recognizable "posterior" depressors close to the midline, but in the left body half, the muscles are slightly less pronounced than in right body half (Figure 4(b)). The "femur" lacks the "posterior" ventral depressors, that is, the paired organization of the intrinsic musculature is here least pronounced, conveying the impression of a normal muscle equipment of an unperturbed femur. "Tibia 1" shows a weakly developed "posterior" depressor in the right body half, whereas it is lacking on the left side, thus resembling the only article with pronounced right/left asymmetry. This is also reflected in the only weakly developed "anterior" depressor of the left half. In contrast, the distally widening "tibia 2" displays again well-separated paired ventral depressors in each body half. Notably, along the midline it possesses an additional longitudinal muscle bundle that has no counterpart in regular legs and serves no obvious function (Figure 4(b)).

Up to "tibia 2", the dorsal extrinsic (Figure 4(c)) and intrinsic (Figure 4(a)) levator muscles of the malformed leg do not show a similarly pronounced paired arrangement as their ventral counterparts. Instead, each body half contributes only an "anterior" levator set, resulting in a normal-looking array of dorsal muscles per article. Only "coxa 1" shows an untypical arrangement, as the dorsal musculature is represented by one set of protractors in each body half, which are presumably nonfunctional without the dorsal joint (Figure 4(c)).

The small anal tubercle contains only one weakly developed muscle bundle in the right body half (Figure 4(c)). It attaches internally to the slit-like cuticular depression, but does not form a fully functional anus musculature (compare to Figure 2(d)).

3.4 | Central nervous system and midgut of the malformed specimen

Apart from the musculature (mesodermal origin), only the central nervous system (ectodermal origin) and the midgut (endodermal origin) were assessed, as the gonads are still in a primordial state in pycnogonids in this developmental stage (Miyazaki & Makioka, 2012; see also Brenneis et al., 2017).

The ventral nerve cord features a well-developed subesophageal ganglion (including the palpal, ovigeral, and first leg neuromeres) as well as the ganglion of trunk segment 2 and the normal-looking ganglion of the malformed trunk segment 3 (Figure 5(c)). The segmental leg nerves of the third trunk ganglion could not be followed in the phalloidin labeling, but our live observation of movement clearly indicate functional innervation of the abnormal leg. There are no traces of a ganglion of trunk segment 4 or of any additional posterior ganglion

FIGURE 3 External morphology of the malformed specimen. SEM micrographs (a,c,d) and volume rendering of cuticular autofluorescence (b). (a) Overview of the specimen, anterodorsal view. Note external articulation of all legs, including the malformed one. Black arrowheads mark a long dorsodistal seta on femur and tibiae 1 and 2 of normally developed legs. (b) Detail of left leg 1, ventral view. The leg shows the typical nine leg articles (compare to Figure 1(d)) and its joints are in normal positions (arrowheads), including their characteristic 90° rotation between coxae 1 and 2 (arrow). (C) Detail of "tibia 2" and separate tarsi and propodi, dorsal view. Arrowheads mark two long dorsal setae at the incompletely fused distal margins of the tibiae 2. (d) Malformed leg, lateral view, posterior to the top, dorsal to the right. Trunk segment 3 and its "lateral process" are not distinctly set off from each other, the latter forming a short unpaired protrusion. "Femur" and the two "tibiae" are shorter than in normally developed legs. Black arrowheads mark a pair of long dorsal setae at the distal end of "tibia 2", with no counterparts on "femur" and "tibia 1". Note rudimentary dorsal anal tubercle at the border of trunk segments 2 and 3. (e) Detail of rudimentary anal tubercle, dorsal view. Note vaguely slit-shaped posterior depression in the cuticle (arrow) but no apparent opening. AF, autofluorescence; ch, cheliphore; cx, coxa; fe, femur; lp, lateral process; mc, main claw; pr, propodus; ta, tarsus; tb, tibia; ts, trunk segment; wl, walking leg

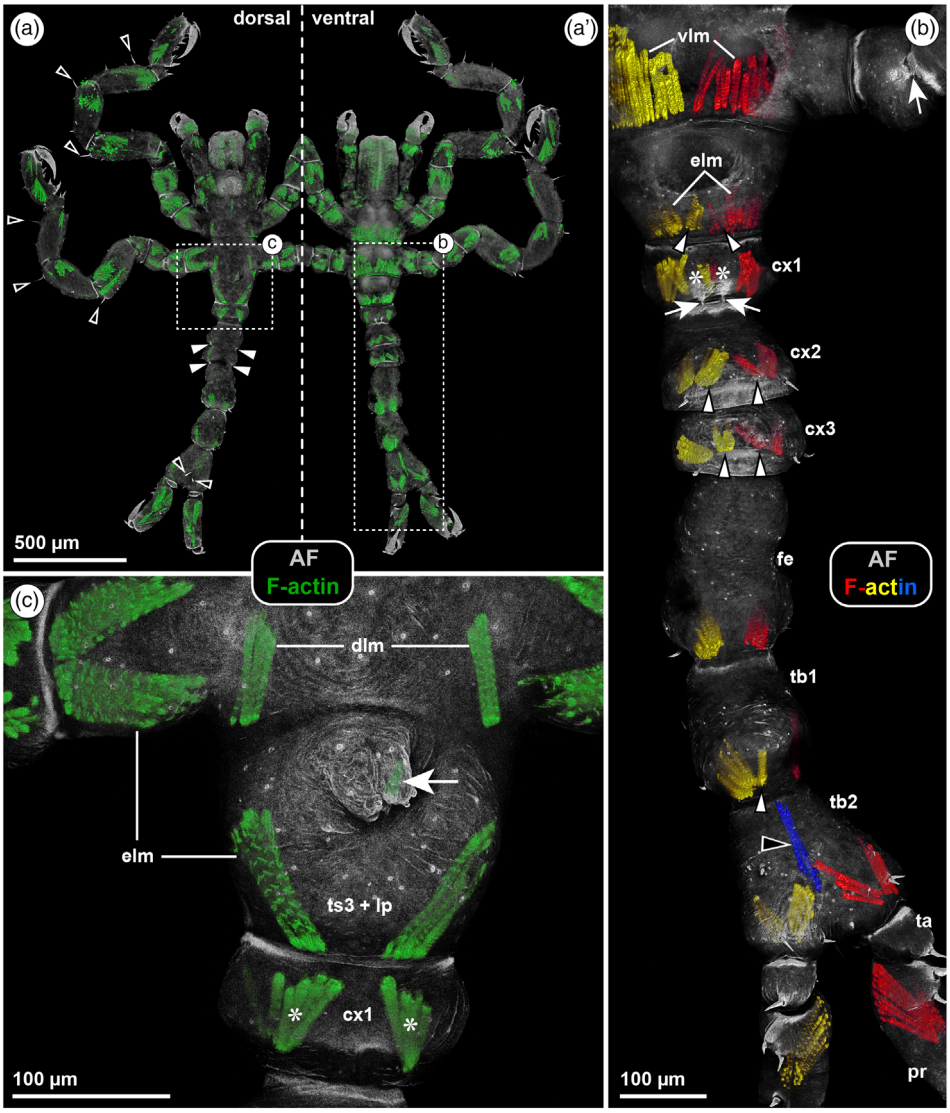

FIGURE 4 Musculature of the malformed specimen. Volume renderings (CLSM scans) showing F-actin labeling (green or differentially colored) and cuticular autofluorescence (gray). (a, a'): Dorsal and ventral overviews of the malformed individual, with normal musculature in body regions and legs anterior to trunk segment 3. Open arrowheads point at prominent dorsodistal setae on the three long articles in normal legs and on "tibia 2" of the malformed leg. Solid arrowheads highlight dorsolateral joints between "coxa 2" and "coxa 3" as well as "coxa 3" and "femur" in the malformed leg. Stippled rectangles indicate regions shown in (b) and (c). (b) Color-coded reconstruction of ventral musculature in trunk segments 2 and 3 and the malformed leg. Red and yellow colors indicate muscles assigned to left and right body halves, respectively. A median longitudinal muscle group (blue color & open arrowhead) in "tibia 2" has no correspondence in a regular leg. Note presence of two ventral joints between "coxa 1" and "coxa 2", as opposed the single joint in leg 2 (arrows). In the three "coxae", the paired structure of the ventral muscles is recognizable, with the respective "posterior" muscle sets adjoining at the midline (asterisks = retractors; arrowheads = depressors). Note less voluminous "posterior" muscles in the left body half. The "femur" lacks the "posterior" depressors completely and "tibia 1" features a weakly developed "posterior" depressor in the right body half only (arrowhead). (c) Reconstruction of musculature at the posterior body pole, dorsal view. Only the "anterior" levators of the dorsal extrinsic leg musculature are developed. Judging by orientation, the muscles in "coxa 1" represent the "anterior" protractors of each body half (asterisks), while the "posterior" retractors and joint(s) are missing. Note a single weakly labeled muscle bundle (arrow) in the right half of the vestigial anal tubercle. AF, autofluorescence; cx, coxa; dlm, dorsal longitudinal trunk musculature; elm, extrinsic leg musculature; lp, lateral process; pr, propodus; ta, tarsus; tb, tibia; ts, trunk segment; vlm, ventral longitudinal trunk musculature

anlagen (Figure 5(c)), which are clearly recognizable in regular first free-living instars (Figure 5(b)) and even in advanced endoparasitic stages prior to emergence from the host (Figure 5(a)).

The midgut was only diffusely labelled by the DRAQ5 staining. Its lumen is displayed as dark central region and the thick and irregular midgut epithelium is light gray with a few more intensely labeled dots indicating cell nuclei (Figure 6(a),(b)). A single midgut diverticulum extends into each normally developed walking leg (Figure 6(a)). The malformed appendage also contains only one unpaired, but slightly thicker diverticulum from "coxa 1" to "tibia 1"

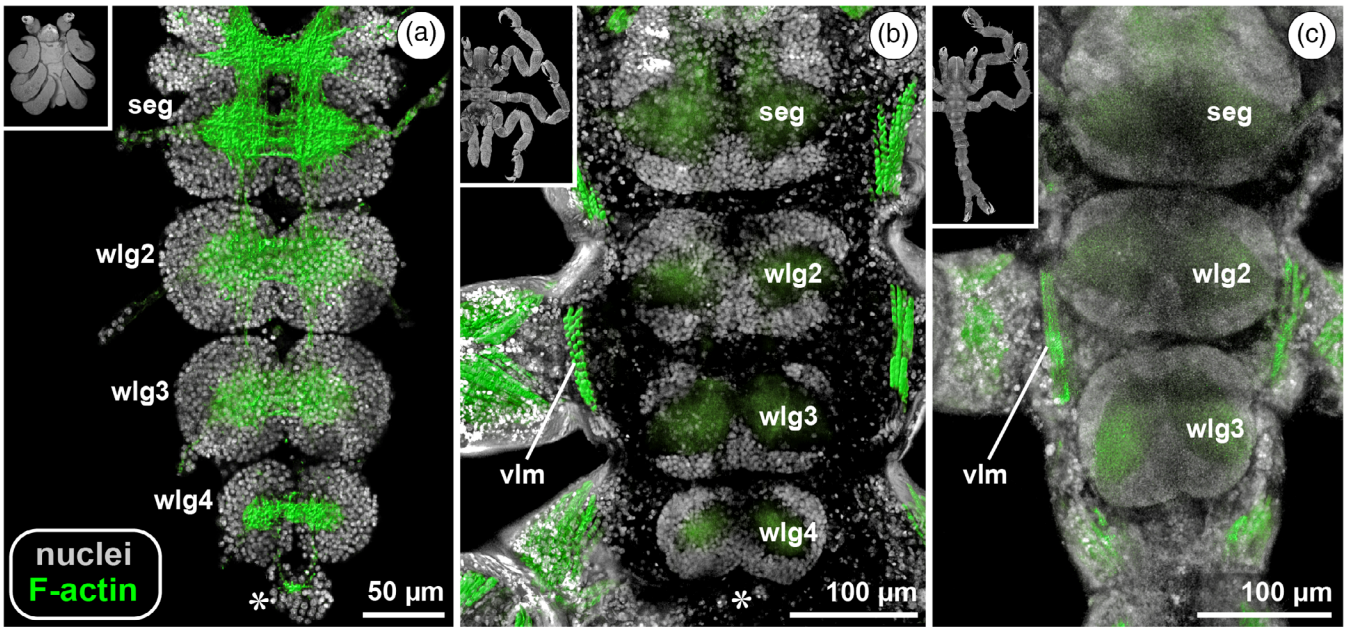

FIGURE 5 Ventral nerve cord in different developmental instars of *P. femoratum*. Volume renderings (CLSM scans) showing F-actin labeling (green) and nuclei (Hoechst or DRAQ5; gray). Filtered oblique slicers applied to reveal internal target structures. Gross anatomy of the ventral nerve cord in a late endoparasitic instar (a), the first free-living instar (b) and the malformed specimen (c), ventral views. Note lack of any central nervous system structures posterior to leg ganglion 3 in the malformed individual. The asterisks highlight transient posterior ganglion anlagen formed during the endoparasitic phase but largely reduced in free-living instars. seg, subesophageal ganglion; vlm, ventral longitudinal trunk musculature; wlg, walking leg ganglion

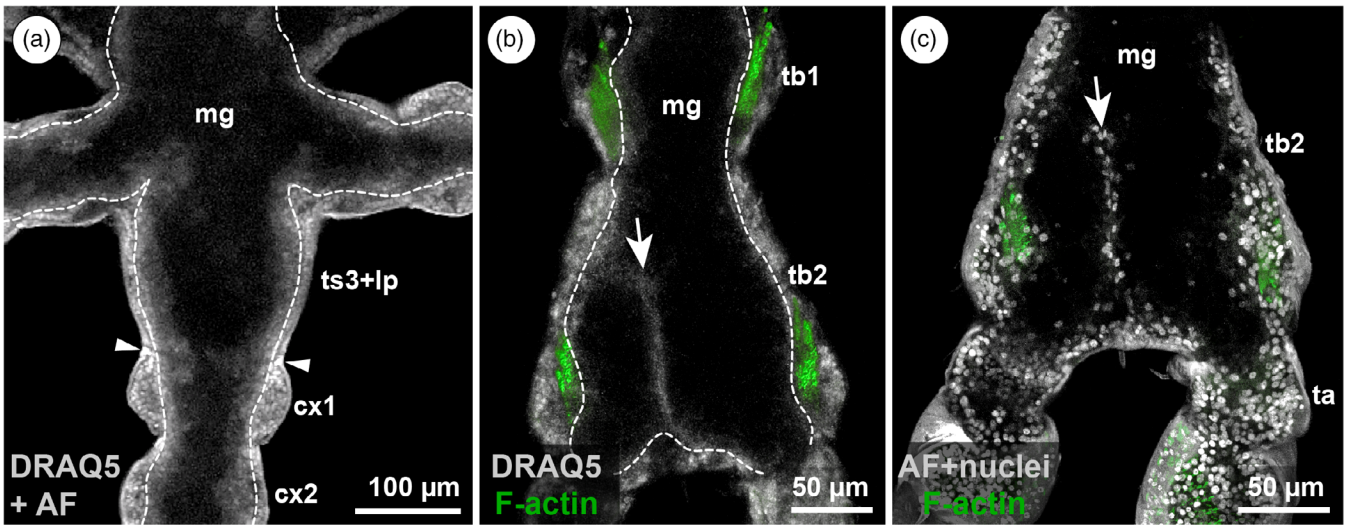

FIGURE 6 Midgut diverticulum of the malformed leg. Volume renderings (CLSM scans) showing F-actin labeling (green) and nuclei (Hoechst or DRAQ5; gray). Filtered oblique slicers applied to reveal internal target structures. (a) Ventral view. A single diverticulum emanates from the midgut (stippled outlines) laterally into each leg 2 and posteriorly into the malformed leg. Arrowheads mark the brightly labeled lateral joints between the "lateral process" and "coxa 1" of the malformed leg. (b) Dorsal view. The midgut diverticulum (stippled outlines) is unpaired up to "tibia 1" but subdivides longitudinally into two lumina (arrow) in "tibia 2". (c) Dorsal view. Hoechst nuclear labeling confirms the cellular nature of the longitudinal subdivision (arrow), representing endodermal midgut epithelium. AF, autofluorescence; cx, coxa; lp, lateral process; mg, midgut; ta, tarsus; tb, tibia; ts, trunk segment

(Figure 6(a),(b)). In the externally bipartite "tibia 2", the midgut diverticulum splits into two corresponding portions (Figure 6(b)), the cellular nature of the slightly oblique subdivision (= midgut epithelium) being confirmed by Hoechst nuclear labeling (Figure 6 (c)). A connection between the midgut and the vestigial anal tubercle could not be traced with certainty.

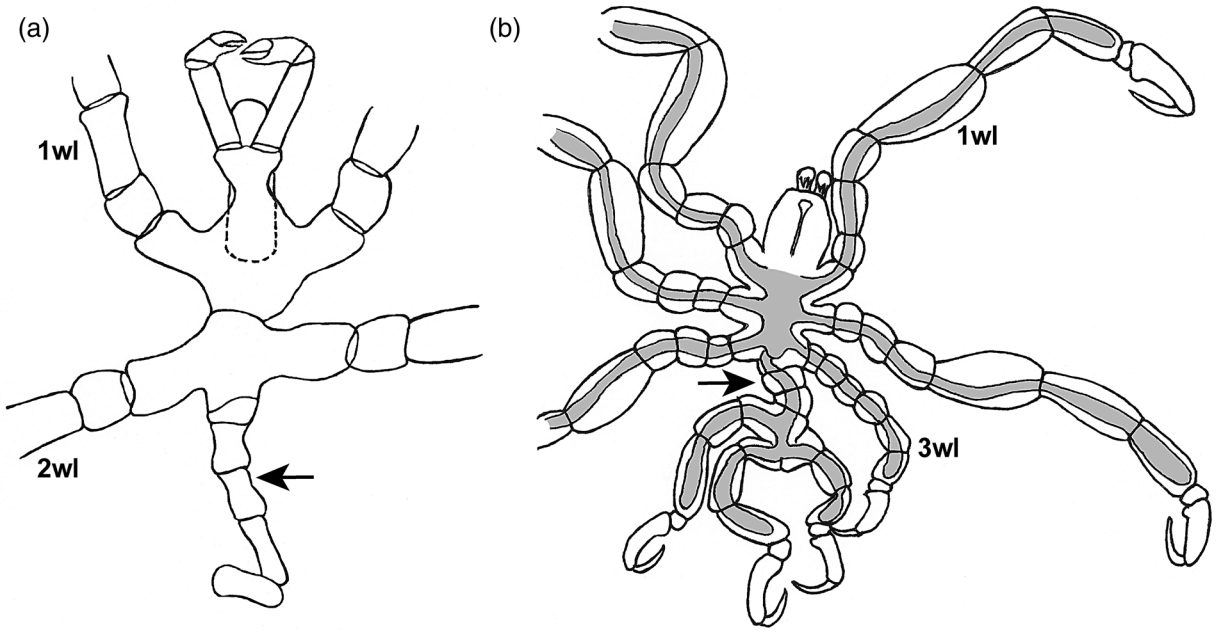

FIGURE 7 Historical accounts of malformed specimens in Phoxichilidiidae. (a) *Phoxichilidium femoratum*. Specimen featuring an unpaired articulated regenerate (arrow) aligned with the anteroposterior body axis after amputation of trunk segments 3 and 4 (modified from Loeb, 1895). (b) *Anoplodactylus petiolatus*. Specimen with a trifurcating leg (arrow) emanating from the posterior pole of the trunk (modified from Schimkewitsch & Dogiel, 1913). wl, walking leg

4 | DISCUSSION

4.1 | Debates in previous studies and backward argumentation

The pattern described here partly resembles the outcome of experiments carried out by Loeb (1895) in *Phoxichilidium femoratum*. Loeb cut specimens in two between the second and third trunk segments. One specimen regenerated a single multi-segmented structure as an extension of the anteroposterior body axis (Figure 7(a)) with a midgut diverticulum present in the proximal part of this regenerate. However, Loeb was insecure whether this regenerate should be interpreted as anal tubercle or rather as incompletely articulated leg, and unfortunately he did not investigate the musculature or the presence of joints to further clarify the nature of the structure. Eventually, however, he favored the idea that it is a combination of the trunk and the anal tubercle (Loeb, 1895). This conclusion was severely criticized by Morgan (1904) who discussed the issue and failed to replicate Loeb's experimental results. He suggested that the regenerate has to represent an incomplete leg, in spite of its unusual alignment with the anteroposterior body axis, because it comprised too many elements for trunk and anal tubercle and lacked any associated segmental limb structures. As illustrated by the pycnogonid specimen in our study, there is indeed the possibility that leg structures can grow out as direct extension of the anteroposterior body axis, which lends further support to Morgan (1904).

However, the observed pattern is not the result of a controlled experiment. Hence, one has to reconstruct the causes and mechanisms that created the observable outcome via backward argumentation, that is, starting with analysis of the "pattern of the malformed structure in order to reconstruct a plausible narrative of a scenario that may have led to the observed result" (Scholtz & Brenneis, 2016, p. 13). In the case of the malformed specimen of *P. femoratum* studied here, there are at least two alternative explanations.

Hypothesis 1. Fusion.

This hypothesis suggests a fusion of leg pair 3 along the posterior margin caused by a lesion of the terminal region of an early endoparasitic instar, presumably similar to instar 4 of *Anoplodactylus eroticus* (Maxmen, 2006), a close relative of *P. femoratum*. The hypothetical injury affected the posteromedian region of the early anlagen of leg 3 and the posterior segment addition zone. This led to a fusion of the posterior parts of the prospective lateral processes and the proximal parts of the outgrowing buds of leg pair 3. With further limb elongation and differentiation, the bilaterally paired arrangement of the muscles developed. Since the limb buds of the third legs were in an early stage, they contained only small primordia of the midgut diverticula (see Alexeeva et al., 2018; Bogomolova & Malakhov, 2003; Okuda, 1940) which were also affected by the injury. Later, one diverticulum entered the posteriorly fused leg pair. This could either be a fused regenerate of the injured diverticulum primordia of leg pair 3 or just an extension of the central midgut, which secondarily branched in the bifurcate tips of the fused limbs. It is known from regenerated pycnogonid limbs that the midgut diverticula also regenerate and grow into

the new limb even if this limb shows a bi- or trifurcation (Figure 7(b); Ohshima, 1942b; Schimkewitsch & Dogiel, 1913; Scholtz & Brenneis, 2016). Furthermore, the lack of competent cells posterior to trunk segment 3 prohibited the formation of trunk segment 4 (including its ganglion) and only a partial differentiation of the dorsal anal tubercle lacking most muscles and probably also an open anus. The fact that the ganglion of the malformed trunk segment 3 is normally differentiated may be explained by a characteristic feature of sea spider development. Typically, the ganglion anlagen of the trunk are formed in advance to the associated segmental limb buds (Alexeeva et al., 2018; Brenneis & Arango, 2019; Brenneis & Scholtz, 2014; Morgan, 1891; Okuda, 1940), which holds also for phoxichilidiids (see Maxmen, 2006). Furthermore, in the last two trunk segments, they are shifted anteriorly with respect to the corresponding limb anlagen. Accordingly, the primordia of these trunk segments represent a semicircular arch with the open side towards the posterior, an arrangement that is conserved even in many adult pycnogonids (Brenneis et al., 2018; Dohrn, 1881; Helfer & Schlottke, 1935; Henry, 1953). Apparently, the injury did not affect the more anterior located ganglion anlage of trunk segment 3, although it was already present. A challenge to this hypothesis poses the vestigial anal tubercle. Its position at the posterior boundary of trunk segment 2 is difficult to explain. Normally, the anal tubercle of *P. femoratum* is located at the dorsoposterior end of trunk segment 4 (Figure 1(b)). If the lesion led to a complete loss of the latter and a median fusion of the lateral processes of trunk segment 3, one would not expect the occurrence of an anal tubercle at all. However, it may be an indication that the dorsal side of trunk segment 3 was also affected and perhaps some cell groups forming the body terminus survived the injury and became anteriorly shifted, when the parts of trunk segment 3 were rearranged.

A "fusion" event like this would be unique for pycnogonids and to our knowledge for arthropods in general. Hence, we found no correspondence in any other report of pycnogonid malformations.

Hypothesis 2. Irregular regeneration.

The second hypothesis favors an irregular regeneration of the posterior appendage. In this case, the injury at the posterior end may have happened at a later developmental stage than in the fusion scenario. According to this alternative scenario, a lesion injury of the terminal region led to the complete loss of trunk segment 4, and most parts of trunk segment 3. During the process of wound healing, formation of a new limb bud was initiated, which grew out of the posterior body pole as extension of the anteroposterior axis. Presumably, limb bud elongation and differentiation into an articulated leg included at least one, if not several molts, as is characteristic for pycnogonids (e.g., Alexeeva et al., 2018; Brenneis et al., 2011). It is possible that the bilateral symmetry of the body superimposed the leg anlage and caused the paired muscle structures (for a discussion of the relationships between body and leg axes see Minelli, 2000). Alternatively, a slight asymmetry led to the irregular regeneration of the third leg of one body side, which only secondarily gained a median position. The assumption of a slight asymmetry is supported by the differently expressed musculature in the two leg halves. In this case, the regenerate underwent a duplication showing the characteristic mirror image pattern of biramous regenerated legs (see Bateson, 1894; Meinhardt, 2008; Scholtz, 2020; Scholtz & Brenneis, 2016). The explanation for the regular ganglion in trunk segment 3 and for the midgut diverticulum pattern is the same as in the first hypothesis.

This second scenario offers the possibility to compare the here described specimen with an example of a malformed adult individual of *Anoplodactylus petiolatus* (Krøyer, 1844), which was described by Schimkewitsch and Dogiel (1913); Figure 7(b)). This specimen possesses three anterior pairs of legs in their normal positions (only the third leg on the left side is a bit smaller). A seventh leg originates underneath the anal tubercle at the posterior end of the trunk as an extension of the central body axis. In contrast to the specimen in our study, this leg is not only bifurcate but trifurcate, again with the characteristic symmetry of triplicate arthropod limbs (Bateson, 1894; Meinhardt, 2008; Scholtz, 2020). Schimkewitsch and Dogiel (1913) interpreted the trifurcate limb as the malformed left walking leg 4, but apart from a slight shift to the left side there is no real evidence for this conclusion.

However, similar to the fusion hypothesis, the small dorsal anal tubercle poses a problem to the irregular regeneration scenario. The suggested complete loss of trunk segment 4 also implies the loss of the anal tubercle. Hence, its *de novo* formation would have to be postulated, but convincing evidence for the ability to regenerate the posterior body pole (including the anus anlage) is not only lacking for pycnogonids but also for arthropods in general (Marruzo & Bortolin, 2013).

4.2 | Perspective

It remains to be experimentally tested which of the proposed scenarios is more realistic. Although pycnogonids are generally considered to show good regenerative abilities for arthropod standards (at least with regard to their legs; Marruzo & Bortolin, 2013), this view remains largely based on anecdotal observations on single, opportunistically collected specimens. To our knowledge, Loeb's (1895) and Morgan's (1904) studies have been the only dedicated experimental approaches to study pycnogonid regenerative abilities, with the exception of scattered incomplete side-notes on leg amputation trials (Helfer & Schlottke, 1935; Schmidt, 1971). Hence, more than a century after Loeb's and Morgan's pioneering work, it would be desirable to perform more systematic regeneration experiments on pycnogonids, focusing on species for which a successful laboratory husbandry has been established in the meantime, such as *Pycnogonum litorale* (see Brenneis et al., 2017). This important prerequisite would help overcome limitations of the previous short-term setups (Loeb, 1895; Morgan, 1904) and additionally afford the opportunity to use some of today's more advanced tools for the study of arthropod development.

ACKNOWLEDGEMENTS

Eric Lovely (Arkansas Tech University) kindly pointed out the locality for *P. femoratum* collection. G.B. is indebted to Barbara Beltz for hosting him in her lab at Wellesley College, MA, during the fluorescent histochemical work of the study. Amanda L. Kohn, Ben J. Lang, Nazar Mashtalir and Dominik Bucher (a.k.a. the Moxie-maniacs) are thanked for their help during several collection trips to Portsmouth, NH. The assistance of Thomas Stach and Peer Martin (Humboldt-Universität zu Berlin) with the SEM is gratefully acknowledged. Marie Hörnig and Jakob Krieger (Universität Greifswald) are thanked for introducing G.B. to X-ray μCT and sharing their knowledge of various Amira features. The comments and suggestions of two anonymous reviewers helped to improve the manuscript. Research was supported by the Deutsche Forschungsgemeinschaft (DFG INST 292/119-1 FUGG and DFG INST 292/120-1 FUGG). Open access funding enabled and organized by Projekt DEAL.

AUTHOR CONTRIBUTIONS

Georg Brenneis: Conceptualization; data curation; formal analysis; funding acquisition; investigation; visualization; writing-original draft. **Gerhard Scholtz:** Formal analysis; writing-original draft.

PEER REVIEW

The peer review history for this article is available at https://publons.com/publon/10.1002/jmor.21303.

DATA AVAILABILITY STATEMENT

The data that support the findings of this study are available from the corresponding author upon reasonable request.

ORCID

Georg Brenneis https://orcid.org/0000-0003-1202-1899

REFERENCES

Adlerz, G. (1888). Bidrag till pantopodernas morfologi och utvecklingshistoria. *Bihang till Kungliga Svenska Vetenskaps-Akademiens Handlingar*, *13*, 1–25.

Alexeeva, N., Bogomolova, E. V., Tamberg, Y., & Shunatova, N. (2017). Oligomeric larvae of the pycnogonids revisited. *Journal of Morphology*, *278*, 1284–1304.

Alexeeva, N., Tamberg, Y., & Shunatova, N. (2018). Postembryonic development of pycnogonids: A deeper look inside. *Arthropod Structure & Development*, *47*, 299–317.

Alexeeva, N., Tamberg, Y., & Shunatova, N. (2019). The (not very) typical protonymphons of *Pycnogonum litorale*. *Journal of Morphology*, *280*, 1370–1392.

Arita, K. (1936). Ein überzähliges Bein einer Pantopoden-Art (*Nymphonella tapetis* Ohshima). *Annotationes Zoologicae Japonense*, *15*, 469–479.

Arnaud, F., & Bamber, R. N. (1987). The biology of Pycnogonida. *Advances in Marine Biology*, *24*, 1–96.

Ballesteros, J. A., Setton, E. V. W., Santibánez López, C. E., Arango, C. P., Brenneis, G., Brix, S., … Sharma, P. P. (2020). Phylogenomic resolution of sea spider diversification through integration of multiple data classes. *Molecular Biology and Evolution*. https://doi.org/10.1093/molbev/msaa228

Bateson, W. (1894). *Materials for the study of variation*. London, UK: MacMillan and Co.

Bergström, J., Stürmer, W., & Winter, G. (1980). *Palaeoisopus*, *Palaeopantopus* and *Palaeothea*, pycnogonid arthropods from the lower Devonian Hunsrück slate, West Germany. *Paläontologische Zeitschrift*, *54*, 7–54.

Bogomolova, E. V., & Malakhov, V. V. (2003). Larvae of sea spiders (Arthropoda, Pycnogonida) from the White Sea. *Entomological Review*, *83*, 222–236.

Bogomolova, E. V., & Malakhov, V. V. (2011). Structure of the body cavity of the sea spider *Nymphon brevirostre* Hodge, 1863 (Arthropoda: Pycnogonida). *Russian Journal of Marine Biology*, *37*, 348–365.

Bouvier, M. E.-L. (1914). Quelques mots sur la variabilité du *Pycnogonum littorale*, Ström. *Journal of the Marine Biological Association of the United Kingdom*, *10*, 207–210.

Brenneis, G. (2016). Pycnogonida (Pantopoda). In A. Schmidt-Rhaesa, S. Harzsch, & G. Purschke (Eds.), *Structure and evolution of invertebrate nervous systems* (pp. 419–427). Oxford, UK: Oxford University press.

Brenneis, G., & Arango, C. P. (2019). First description of epimorphic development in Antarctic Pallenopsidae (Arthropoda, Pycnogonida) with insights into the evolution of the four-articled sea spider cheliphore. *Zoological Letters*, *5*, 4.

Brenneis, G., & Scholtz, G. (2014). The 'ventral organs' of Pycnogonida (Arthropoda) are neurogenic niches of late embryonic and post-embryonic nervous system development. *PLoS One*, *9*(4), e95435.

Brenneis, G., Arango, C. P., & Scholtz, G. (2011). Morphogenesis of *Pseudopallene sp*. (Pycnogonida, Callipallenidae) II: Postembryonic development. *Development Genes and Evolution*, *221*, 329–350.

Brenneis, G., Bogomolova, E. V., Arango, C. P., & Krapp, F. (2017). From egg to "no-body": An overview and revision of developmental pathways in the ancient arthropod lineage Pycnogonida. *Frontiers in Zoology*, *14*, 6.

Brenneis, G., Scholtz, G., & Beltz, B. S. (2018). Comparison of ventral organ development across Pycnogonida (Arthropoda, Chelicerata) provides evidence for a plesiomorphic mode of late neurogenesis in sea spiders and myriapods. *BMC Evolutionary Biology*, *18*, 47.

Charmantier-Daures, M., & Vernet, G. (2004). Moulting, autotomy, and regeneration. In J. Forest, J. C. von Vaupel Klein, & F. R. Schram (Eds.), *Treatise on zoology—Anatomy, taxonomy, biology, the Crustacea* (Vol. 1, pp. 161–255). Leiden: Brill.

Dencker, D. (1974). Das Skeletmuskelsystem von *Nymphon rubrum* Hodge, 1862 (Pycnogonida: Nymphonidae). *Zoologische Jahrbücher. Abteilung für Anatomie und Ontogenie der Tiere*, *93*, 272–287.

Dogiel, V. (1911). Ein interessanter Fall von atavistischer Mißbildung bei einer Pantopodenlarve. *Zoologischer Anzeiger*, *38*, 321–323.

Dogiel, V. (1913). Embryologische studien an pantopoden. *Zeitschrift für Wissenschaftliche Zoologie*, *107*, 575–741.

Dohrn, A. (1881). *Die Pantopoden des Golfes von Neapel und der angrenzenden Meeres-Abschnitte*. Leipzig: Verlag von Wilhelm Engelmann.

Dunlop, J. A., & Lamsdell, J. C. (2017). Segmentation and tagmosis in Chelicerata. *Arthropod Structure & Development*, *46*, 395–418.

Elliott, S. A., & Sánchez Alvarado, A. (2018). Planarians and the history of animal regeneration: Paradigm shifts and key concepts in biology. In J. C. Rink (Ed.), *Planarian regeneration: Methods and protocols, methods in molecular biology* (Vol. 1774, pp. 207–239). Totowa: Humana Press.

Galli, L., Colasanto, E., Betti, F., & Capurro, M. (2019). Pycnogonids (Arthropoda: Pycnogonida) of Portofino, Ligurian Sea (North-Western Mediterranean Sea). *The European Zoological Journal*, *89*, 241–248.

Gaubert, P. (1892). Autotomie chez les Pycnogonides. *Bulletin de la Société Zoologique de France*, *17*, 224.

Gordon, I. (1932). Pycnogonida. *Discovery Report*, *6*, 1–138.

Hedgpeth, J. W. (1947). On the evolutionary significance of the Pycnogonida. *Smithsonian Miscellaneous Collections*, *106*, 1–53.

Helfer, H., & Schlottke, E. (1935). *Abteilung IV, Buch 2* Pantopoda. Dr. H. G. Bronns Klassen und Ordnungen des Tierreichs (Vol. 5). Leipzig: Akademische Verlagsgesellschaft mbH.

Henry, L. M. (1953). The nervous system of the Pycnogonida. *Microentomology*, *18*, 16–36.

King, P. E. (1973). *Pycnogonids*. London, UK: Hutchinson & Co.

Korschelt, E. (1907). *Regeneration und transplantation. Jena: Gustav*. Verlag: Fischer.

Lebour, M. V. (1916). Notes on the life history of *Anaphia petiolata* (Kröyer). *Journal of the Marine Biological Association of the United Kingdom*, *11*, 51–56.

Lebour, M. V. (1945). Notes on the Pycnogonida of Plymouth. *Journal of the Marine Biological Association of the United Kingdom*, *26*, 139–165.

Loeb, J. (1895). Bemerkungen über regeneration. (1. Über die Regeneration des Rumpfes bei Pantopoden. 2. Zur Theorie der Regenerationserscheinungen). *Archiv für Entwicklungsmechanik der Organismen*, *2*, 250–256.

Lovely, E. C. (2005). The life history of *Phoxichilidium tubulariae* (Pycnogonida: Phoxichilidiidae). *Northeastern Naturalist*, *12*, 77–92.

Maruzzo, D., Bonato, L., Brena, C., Fusco, G., & Minelli, A. (2005). Appendage loss and regeneration in arthropods: A comparative view. In S. Koenemann & R. A. Jenner (Eds.), *Crustacea and arthropod relationships* (pp. 215–245). Boca Raton: CRC Press.

Marruzo, D., & Bortolin, F. (2013). Arthropod regeneration. In A. Minelli, G. Boxshall, & G. Fusco (Eds.), *Arthropod biology and evolution. Molecules, development, morphology* (pp. 149–169). Berlin Heidelberg: Springer-Verlag.

Maxmen, A. (2006). Pycnogonid development and the evolution of the arthropod body plan. PhD thesis, Harvard University, Cambridge, MA.

Meinhardt, H. (2008). Models of biological pattern formation: From elementary steps to the organization of embryonic axes. *Current Topics in Developmental Biology*, *81*, 1–63.

Minelli, A. (2000). Limbs and tail as evolutionarily diverging duplicates of the main body axis. *Evolution and Development*, *2*, 157–165.

Miyazaki, K., & Makioka, T. (2012). Postembryonic development of the female reproductive system in the pycnogonid *Propallene longiceps* (Pycnogonida, Callipallenidae). *Invertebrate Reproduction and Development*, *56*, 287–292.

Mochizuki, Y., & Miyazaki, K. (2017). Postembryonic development of the sea spider *Ammothella biunguiculata* (Pycnogonida, Ammotheidae) endoparasitic to an actinian *Entacmaea quadricolor* (Anthozoa, Stichodactylidae) in Izu peninsula, Japan. *Invertebrate Reproduction and Development*, *61*, 189–199.

Morgan, T. H. (1891). A contribution to the embryology and phylogeny of the pycnogonids. *Studies from the Biological Laboratory of the Johns Hopkins University Baltimore*, *5*, 1–76.

Morgan, T. H. (1904). Notes on regeneration. *Biological Bulletin*, *6*, 159–172.

Ohshima, H. (1942a). Six-legged pantopod, an extraordinary case of hypomery in arthropods. *Proceedings of the Imperial Academy*, *18*, 257–262.

Ohshima, H. (1942b). A remarkable case of malformed appendages in a pantopod, *Nymphonella tapetis*. *Proceedings of the Imperial Academy*, *18*, 520–523.

Okuda, S. (1940). Metamorphosis of a pycnogonid parasitic in a hydromedusa. *Journal of the Faculty of Science, Hokkaido Imperial University, Series*, *6*(7), 73–86.

Poschmann, M., & Dunlop, J. (2006). A new sea spider (Arthropoda: Pycnogonida) with a flagelliform telson from the lower Devonian Hunsrück slate, Germany. *Palaeontology*, *49*, 983–989.

Przibram, H. (1909). *Experimental-Zoologie, 2. Regeneration (Wieder-Erzeugung)*. Leipzig: Franz Deuticke.

Schimkewitsch, W., & Dogiel, V. (1913). Ueber Regeneration bei Pantopoden. *Bulletin de l'Académie Impérial des Sciences de St.-Pétersbourg, VI, Serié*, *7*, 1147–1156.

Schmidt, H.-W. (1971). Die Beeinflussung der Häutungen von *Pycnogonum litorale* (Ström) durch exogene und endogene Faktoren. *Oecologia*, *7*, 249–261.

Scholtz, G. (2020). Duplicated, twisted, and in the wrong place: Patterns of malformation in crustaceans. In K. Anger, S. Harzsch, & M. Thiel (Eds.), *Developmental biology and larval ecology* The natural history of the Crustacea (Vol. 7, pp. 112–142). New York: Oxford University Press.

Scholtz, G., & Brenneis, G. (2016). A specimen of *Pycnogonum litorale* (Arthropoda, Chelicerata, Pycnogonida) with a supernumerary leg is in agreement with the 'boundary model' of appendage formation. *The Science of Nature*, *103*, 13.

Siveter, D. J., Sutton, M. D., Briggs, D. E. G., & Siveter, D. J. (2004). A Silurian sea spider. *Nature*, *431*, 978–980.

Tiozzo, S., & Copley, R. R. (2015). Reconsidering regeneration in metazoans: An evo-devo approach. *Frontiers in Ecology and Evolution*, *3*, 67.

Tjønneland, A., Kryvi, H., Ostnes, J. P., & Økland, S. (1985). The heart ultrastructure in two species of pycnogonids, and its phylogenetic implications. *Zoologica Scripta*, *14*, 215–219.

Trembley, A. (1744). *Mémoires, Pour Servir à l'Histoire d'un Genre de Polypes d'Eau Douce, à Bras en Forme de Cornes*. Leiden: Verbeek.

Woods, H. A., Lane, S. J., Shishido, C., Tobalske, B. W., Arango, C. P., & Moran, A. L. (2017). Respiratory gut peristalsis by sea spiders. *Current Biology*, *27*, R638–R639.

How to cite this article: Brenneis G, Scholtz G. A postlarval instar of *Phoxichilidium femoratum* (Pycnogonida, Phoxichilidiidae) with an exceptional malformation. *Journal of Morphology*. 2021;282: 278–290. https://doi.org/10.1002/jmor.21303